RAA 2017 Vol. **17** No. **9**, 90 (10pp) doi: 10.1088/1674–4527/17/9/90

http://www.raa-journal.org *http://iopscience.iop.org/raa*

***R**esearch in*
***A**stronomy and*
***A**strophysics*

Comparisons of Jet Properties between GeV Radio Galaxies and Blazars

Zi-Wei Xue[1,2], Jin Zhang[1,3,4], Wei Cui[3], En-Wei Liang[4] and Shuang-Nan Zhang[1,5,2]

[1] Key Laboratory of Space Astronomy and Technology, National Astronomical Observatories, Chinese Academy of Sciences, Beijing 100012, China; *jinzhang@bao.ac.cn*
[2] University of Chinese Academy of Sciences, Beijing 100049, China
[3] Department of Physics and Astronomy, Purdue University, West Lafayette, IN 47907, USA
[4] Guangxi Key Laboratory for Relativistic Astrophysics, Department of Physics, Guangxi University, Nanning 530004, China
[5] Key Laboratory of Particle Astrophysics, Institute of High Energy Physics, Chinese Academy of Sciences, Beijing 100049, China

Received 2016 December 27; accepted 2017 April 26

Abstract We compile a sample of spectral energy distributions (SEDs) of 12 GeV radio galaxies (RGs), including eight FR I RGs and four FR II RGs. These SEDs can be represented with the one-zone leptonic model. No significant unification, as expected in the unification model, is found for the derived jet parameters between FR I RGs and BL Lacertae objects (BL Lacs) and between FR II RGs and flat spectrum radio quasars (FSRQs). However, on average FR I RGs have a larger $\gamma_{\rm b}$ (break Lorentz factor of electrons) and lower B (magnetic field strength) than FR II RGs, analogous to the differences between BL Lacs and FSRQs. The derived Doppler factors (δ) of RGs are on average smaller than those of blazars, which is consistent with the unification model such that RGs are the misaligned parent populations of blazars with smaller δ. On the basis of jet parameters from SED fits, we calculate their jet powers and the powers carried by each component, and compare their jet compositions and radiation efficiencies with blazars. Most of the RG jets may be dominated by particles, like BL Lacs, not FSRQs. However, the jets of RGs with higher radiation efficiencies tend to have higher jet magnetization. A strong anticorrelation between synchrotron peak frequency and jet power is observed for GeV RGs and blazars in both the observer and co-moving frames, indicating that the "sequence" behavior among blazars, together with the GeV RGs, may be intrinsically dominated by jet power.

Key words: galaxies: active — galaxies: general — galaxies: jets — gamma rays: galaxies — radiation mechanisms: non-thermal

1 INTRODUCTION

Radio galaxies (RGs) belong to a sub-class of active galactic nuclei (AGNs). It was 40 years ago that Fanaroff & Riley (1974) classified RGs into two groups: Fanaroff & Riley Class I (FR I) and Class II (FR II) RGs according to their radio morphology; FR I RGs are core-dominated with "edge-dimmed" radio lobes and FR II RGs are lobe-dominated with "edge-brightened" radio lobes. The classification of radio morphology for RGs is consistent with their radio power distinction: RGs with radio powers lower than 10^{32} erg s^{-1} Hz^{-1} at 408 MHz exhibit almost exclusively FR I morphologies while RGs with radio powers higher than 10^{34} erg s^{-1} Hz^{-1} at 408 MHz show almost exclusively FR II morphologies (Zirbel & Baum 1995). However, in both classifications of radio power and radio morphology, there is a considerable overlap over which RGs can be identified as either an FR I or an FR II RG (Baum et al. 1988; Owen & Laing 1989; Morganti et al. 1993; Zirbel & Baum 1995). Besides the differences in radio power and radio morphology, the strong dichotomy of RGs in optical proper-

ties has also been studied by many authors (e.g., Zirbel & Baum 1995; Buttiglione et al. 2009; Baldi & Capetti 2009): strong emission lines occur in the more powerful FR II RGs, but weaker FR I RGs tend to have no emission line. FR I and FR II RGs may also correspond to low-excitation RGs and high-excitation RGs, respectively, although the low/high-excitation RGs do not have one-to-one correspondence with their corresponding FR I/FR II categories (Hine & Longair 1979; Laing et al. 1994; Hardcastle et al. 2009). FR I and FR II RGs may have intrinsically different accretion modes (e.g., Wu & Cao 2008; Xu et al. 2009), which may also be unified with BL Lacertae objects (BL Lacs) and flat spectrum radio quasars (FSRQs, Xu et al. 2009; Zhang et al. 2014, 2015). The physical reasons for the RG division are still unclear and are also highly debated. However, the fueling mechanism and merging history may play important roles (Hardcastle et al. 2007; Saripalli 2012).

So far, only four FR I RGs have been detected at the very high energy (VHE) γ-ray band (TeV band), i.e., M87 (Aharonian et al. 2003), Cen A (Aharonian et al. 2009), IC 310 (Aleksić et al. 2010) and NGC 1275 (Aleksić et al. 2012). The first confirmed GeV RG was Cen A, which was the only GeV source not belonging to the blazar class in the Third EGRET Catalog of High Energy Gamma-ray Sources (Hartman et al. 1999). Now there are 14 RGs detected at the GeV band with *Fermi*/LAT (Ackermann et al. 2015). The γ-ray emission has been detected and confirmed in the radio lobes of Cen A (Abdo et al. 2010c), which was the first detection of γ-ray emission in large-scale extended regions of AGNs. It also confirmed that there are detectable γ-ray emission by *Fermi*/LAT in the large-scale jets associated with AGNs (Zhang et al. 2009, 2010). Hence the investigation of radiation mechanisms and the locations of γ-ray emission for GeV RGs is very important.

It is well known that most of the confirmed GeV AGNs are blazars (Ackermann et al. 2015), which are divided into BL Lacs and FSRQs according to the strength of optical emission lines. Their spectral energy distributions (SEDs) are dominated by their jet emission and can be explained with the one-zone leptonic models (e.g., Maraschi et al. 1992; Sikora et al. 1994; Ghisellini et al. 1996, 2009; Sikora et al. 2009; Zhang et al. 2012, 2014, 2015; Chen et al. 2012; Liao et al. 2014). The observed SEDs of RGs resemble those of blazars; they show a bimodal feature and can also be explained well by the one-zone leptonic models (Abdo et al. 2009a,b; Aleksić et al. 2014; Fukazawa et al. 2015). According to the unification models for radio loud (RL) AGNs, BL Lacs are associated with FR I RGs, whereas FSRQs are usually linked with FR II RGs (Urry & Padovani 1995), i.e., RGs are the parent populations of blazars with large viewing angles and small Doppler factors (δ). Based on the large sample, we have investigated the jet properties of GeV blazars in our previous works (Zhang et al. 2012, 2014, 2015). Studying the jet properties in different Doppler amplification systems and comparing jet properties between blazars and GeV RGs in both the observer and comoving frames are important for understanding the jet physics and unification models.

In this paper, we compile a sample of SEDs for GeV RGs to study the radiation mechanisms and physical properties of their jets, and explore the unification model of RL AGNs by comparing their jet properties with those of a blazar sample. The sample and observed SEDs of GeV RGs are presented in Section 2. The model and SED fitting are described in Section 3. Comparisons of jet properties between GeV RGs and blazars are presented in Section 4. A summary is given in Section 5.

2 SAMPLE AND DATA

Fourteen RGs with confirmed redshift have been detected with *Fermi*/LAT (Ackermann et al. 2015). The core radiation of Fornax A is very weak compared with its lobe, so the GeV emission of Fornax A may originate from the lobes (McKinley et al. 2015). For IC 310, there are no observational data available at the lower-energy band, and the GeV–TeV spectra of this source cannot be represented with the simple one-zone leptonic model, as shown in figure 5 in Aleksić et al. (2014). Therefore 12 GeV RGs with observed SEDs are included in our sample; eight FR I RGs (Cen A, NGC 1275/3C 84, M87, Cen B, PKS 0625–35, NGC 6251, NGC 1218 and 3C 120) and four FR II RGs (3C 207, 3C 380, 3C 111 and Pictor A). Their SEDs are collected and compiled from the literature and the NASA/IPAC Extragalactic Database (NED)[1], as shown in Figure 1; the simultaneously or quasi-simultaneously observed data are presented as red solid symbols while the non-simultaneously observed data are marked as black open symbols or

[1] Note that the data taken from NED for 3C 207 and 3C 380 should be the total emission of sources, including emission from large-scale jets, which would result in the overestimation of synchrotron radiation for the two sources.

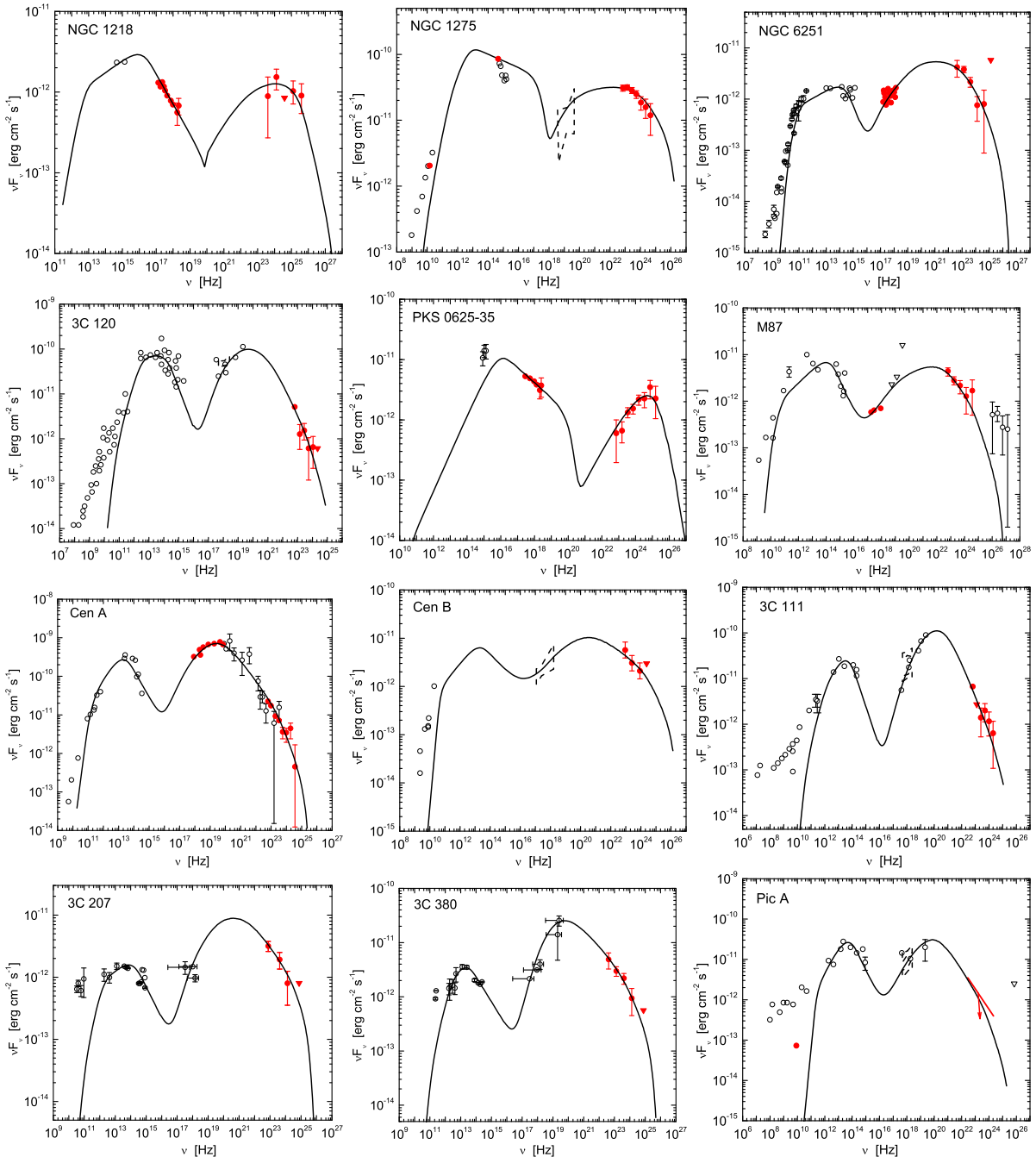

Fig. 1 The observed SEDs with model fitting lines for the 12 RGs in our sample. The simultaneously or quasi-simultaneously observed data are represented as red solid symbols while the non-simultaneously observed data are marked as black open symbols or dashed lines. The triangles are upper limits. The references for data on each source are given in Table 1.

dashed lines. The references for data on each source are given in Table 1.

3 SED MODELING AND RESULTS

As shown in Figure 1, the observed SEDs of RGs are similar to those of blazars and are double peaked. The observed SEDs of blazars can be explained with the one-zone leptonic model and this model is also used to reproduce the SEDs of RGs by many authors, e.g., the synchrotron self-Compton (SSC) scattering process (Abdo et al. 2009a; Migliori et al. 2011; Fukazawa et al. 2015) and external inverse Compton (EC) scattering process

Table 1 SED Fitting Results

Source	z	δ	B (G)	Δt (h)	N_0 (cm^{-1})	p_1	p_2	$\gamma_{\rm min}$	$\gamma_{\rm b}$	$\gamma_{\rm max}$ ($\times\gamma_{\rm b}$)	θ (°)	Re	$\log P_{\rm jet}$ ($\mathrm{erg\ s}^{-1}$)	$\log P_{\rm cav}$ ($\mathrm{erg\ s}^{-1}$)
(1)	(2)	(3)	(4)	(5)	(6)	(7)	(8)	(9)	(10)	(11)	(12)	(13)	(14)	(15)
NGC 1218	0.029	5.6	0.23	24	6.5E5	2.7	3.74	800	5.0E4	100	10.2	F15	42.99	43.79
NGC 1275	0.0179	5.8	0.15	168	1.4E1	1.4	3.2	250	1.3E3	200	9.9	A09a	44.31	43.34
NGC 6251	0.02471	7.8	0.02	24	5.3E6	2.7	4.3	300	1.6E4	10	7.3	M11	44.95	43.64
3C 120	0.033	1.8	3.7	120	8.0E6	2.76	4.76	260	1.9E3	50	31.8	K11	44.54	
PKS 0625–35	0.055	4.9	1.2	24	9.5E1	1.74	3.5	1	2.0E4	100	11.7	F15	43.42	
M87	0.00428	3.0	0.1	48	2.1E5	2.42	4.3	180	1.0E4	100	19.1	A09b	43.58	43.79
Cen A	0.00183	1.2	4.1	24	6.1E4	1.56	4.38	100	9.1E2	100	47.7	A10b	43.36	43.37
Cen B	0.0129	4.8	0.1	24	1.9E5	2.2	3.7	1	3.0E3	100	11.9	K13	44.07	
3C 111	0.0485	4.7	0.45	24	2.8E4	1.7	4.8	300	2.0E3	100	12.2	K11	44.63	44.05
3C 207	0.681	9.8	0.42	24	7.9E6	2.56	4	300	3.3E3	100	5.8	A10a; NDE	45.53	
3C 380	0.692	8.0	0.9	24	2.1E5	1.84	3.92	300	1.0E3	100	7.2	A10a; NDE	45.66	45.56
Pic A	0.0351	2.5	4.2	24	1.6E4	1.6	4.42	1	1.0E3	100	22.9	K11	43.88	

Notes: θ: Derived viewing angle. Re: the references for SED data — F15: Fukazawa et al. (2015); A09a: Abdo et al. (2009a); K11: Kataoka et al. (2007); A10a: Abdo et al. (2010a); NED: NASA/IPAC Extragalactic Database; A09b: Abdo et al. (2009b); A10b: Abdo et al. (2010b); M11: Migliori et al. (2011); K13: Katsuta et al. (2013). $\log P_{\rm jet}$: For PKS 0625–35, Cen B and Pic A, we take $\gamma_{\rm min} = 300$ to calculate their jet powers, which is the median (the mean is $\gamma_{\rm min} = 310$) of the other nine RGs. $\log P_{\rm cav}$: The cavity kinetic powers of RGs in Meyer et al. (2011).

(for M87, Cui et al. 2012). Although a more complex model with more parameters may produce a better fit to the SEDs of some RGs (e.g., Tavecchio & Ghisellini 2014), we prefer to use a simple model to fit the SEDs and to perform a statistical analysis of the jet properties on the basis of fitting results, and then compare their jet properties with those of blazars in our previous works (Zhang et al. 2012, 2014, 2015). Hence the one-zone leptonic model is used to fit the observed SEDs of these GeV RGs in this paper, where the model includes synchrotron radiation and the SSC process. According to the unification models, the FR I and FR II RGs are parent populations of BL Lacs and FSRQs, respectively, and FR II RGs generally have stronger emission lines than FR I RGs, similar to FSRQs. The inverse Compton scattering of photons from the broad-line region (BLR or torus) by relativistic electrons in jets is widely used to explain the gamma-ray emission of FSRQs. Different from FSRQs, the radiations of FR II RGs in both X-ray and GeV bands can be explained well with one SSC component, hence we do not consider the EC/BLR process for FR II RGs during the SED fitting in this paper[2].

There are nine parameters in this model. The radiation region is assumed to be a homogenous sphere with radius R, magnetic field strength B and Doppler factor δ. The radius is obtained with $R = \delta c \Delta t/(1+z)$, where Δt is the variability timescale and listed in Table 1, c is the speed of light and z is the redshift of each source. Similar to blazars, the GeV RGs have different variability timescales in different energy bands (e.g., Aleksić et al. 2014). So, we use the variability timescale at the γ-ray band to constrain the emission region scale. For RGs which have no timescale available in the literature, we take $\Delta t = 1\,\mathrm{d}$. The electron distribution is taken as a broken power law, which is characterized by an electron density parameter (N_0), a break energy $\gamma_{\rm b}$ and indices (p_1 and p_2) in the range of $\gamma_{\rm e}$ [$\gamma_{\rm min}$, $\gamma_{\rm max}$].

There are not enough simultaneous observational data to constrain the parameters as done for blazars in our previous works (Zhang et al. 2012, 2014, 2015), so the goodness of SED fitting is assessed visually. During the process of SED fitting, p_1 and p_2 are derived with spectral indices of the observed SEDs as reported by Zhang et al. (2012). $\gamma_{\rm max}$ is fixed at $100\gamma_{\rm b}$ and sometimes slightly varies to fit the SEDs. $\gamma_{\rm min}$ varies from the minimum value of unity until it can explain the SEDs well. The derived values of $\gamma_{\rm min}$, $\gamma_{\rm b}$, N_0, B and δ are visually assessed, and may thus not be unique. The Klein–Nishina effect and the absorption of high energy gamma-ray photons by extragalactic background light (Franceschini et al. 2008) are also taken into account in our model calculations. The results of SED fitting are shown in Figure 1, and the derived model parameters are reported in Table 1.

[2] We checked another case, taking the EC/BLR process into account during the SED fitting for the four FR II RGs. In this scenario, we will obtain a smaller δ value and a larger B value, but a similar Γ value for the four FR II RGs, and the following results in our paper still hold.

We find that six SEDs of RGs in our sample are also explained with the one-zone leptonic model by other authors (Fukazawa et al. 2015; Abdo et al. 2009a,b, 2010b; Migliori et al. 2011), and thus we compare the derived parameters with those reported in the literature for these sources. Since different sizes of the radiation region are taken for these SEDs, the derived parameter values are also slightly different. On the other hand, the model parameters are not independent, as discussed in Zhang et al. (2012). For example, B and δ are dependent on each other, i.e., $B \propto \delta^{-2}$ to δ^{-3}, which is also consistent with the theoretical result in Tavecchio et al. (1998). Tighter constraints on B and δ would be obtained if the two peaks in the SEDs can be constrained well with the observational data (Zhang et al. 2012).

A simultaneous SED provides the constraint on model parameters at a given state, and then provides a snapshot of the emitting population of particles at that time (Zhang et al. 2014, see also Bartoli et al. 2016). Note that observational data from the radio to γ-ray band of our sample sources are not totally simultaneous. The variation of flux at any energy band would result in different values of model parameters (see also Fukazawa et al. 2016). Although a jet origin of the observed X-ray emission is suggested for some sources (Fukazawa et al. 2015), some RGs may also have strong emission from the accretion disk (Kataoka et al. 2007; Tanaka et al. 2015), and thus their optical and X-ray emission may not completely come from jet radiation. However, we cannot avoid these effects with the limited observational data and also do not consider these effects in the following discussion.

4 COMPARISONS OF JET PROPERTIES BETWEEN GEV RGS AND BLAZARS

We have studied the jet properties of GeV blazars in our previous works (Zhang et al. 2012, 2014, 2015). It is thought that RGs are the parent populations of blazars (Urry & Padovani 1995), hence we compare the physical properties of jets between GeV RGs and blazars in this section, where the data of blazars are taken from Zhang et al. (2012, 2014, 2015). For BL Lacs, only the ones whose jet parameters can be constrained by SED fitting in Zhang et al. (2012) are considered and then there are 24 SEDs as cited in Zhang et al. (2014). For 30 FSRQs, we take the data in Zhang et al. (2015)[3] for the same source in Zhang et al. (2014, 2015). Note that there are only 12 RGs in our sample, including eight FR I RGs and four FR II RGs, so the sample of RGs is very limited.

4.1 Jet Parameters

The distributions of derived jet parameters by SED fitting are shown in Figure 2. For most of the GeV RGs, the minimum energies of electrons ($\gamma_{\rm min}$) in jets are higher than unity as given in Figure 2(a), similar to blazars (Zhang et al. 2012, 2014, 2015). The $\gamma_{\rm b}$ distributions for both FR I and FR II RGs roughly cover the intermediate region of BL Lacs and FSRQs, but on average FR I RGs have larger $\gamma_{\rm b}$ than FR II RGs, as given in Figure 2(b), which is also observed between FSRQs and BL Lacs. The magnetic field strength of RGs is lower than that of FSRQs and more similar to that of BL Lacs, but on average FR II RGs have higher B than FR I RGs, as presented in Figure 2(c). The δ values for most of the RGs are lower than those of blazars, as shown in Figure 2(d). This is consistent with the unification model of RL AGNs in which RGs are the misaligned parent populations of blazars with smaller Doppler factors. However, the δ values of some RGs are similar to those of blazars with $\delta \sim 10$, and these RGs with larger Doppler factors may also have small viewing angles of jets like blazars. Hence, maybe only a fraction of RGs that are thought to be the parent population of blazars have been detected in the VHE γ-ray band (Aharonian et al. 2006, 2009; Aleksić et al. 2012; Tavecchio & Ghisellini 2014).

Note that if the viewing angle is larger than the opening angle of the jet, the one-zone leptonic model would not be able to explain the observational data of blazars, as discussed in Zhang et al. (2015). Hence, the viewing angle should be smaller than the opening angle of the jet in blazars, and the probability is highest when looking at the jet at the angle of $1/\Gamma$, where Γ is the bulk Lorenz factor. When the viewing angle (θ) is equal to the opening angle ($1/\Gamma$) of a jet, we obtain $\Gamma = \delta$ and then we can derive the values of viewing angle[4] with the δ values. The derived values of viewing angle are also given in Table 1. θ ranges from $\sim 5^\circ$ to $\sim 48^\circ$ with a mean of $\sim 16^\circ$. With the derived Doppler factors by flux density variation at the radio band and the apparent jet speed, Hovatta et al. (2009) calculated the viewing angles of six RGs (III ZW2, 3C 84, 3C 111, 3C 120, 3C 380 and OW 637), which range from $\sim 7^\circ$ to $\sim 40^\circ$ with

[3] PKS 2142–758 in Zhang et al. (2015) is removed from our sample for the same reason as reported in Zhu et al. (2016).

[4] For RGs, it should be the lower limit of viewing angle.

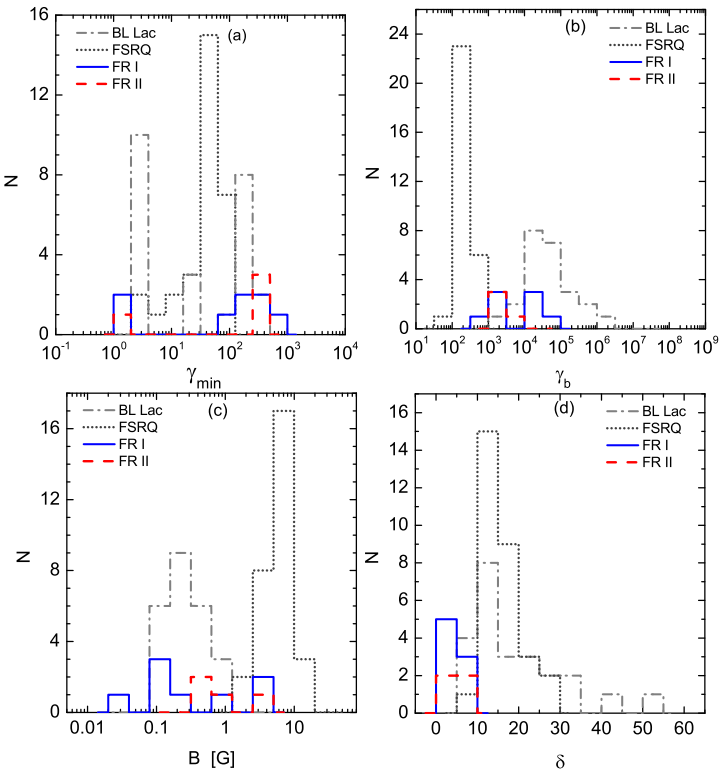

Fig. 2 Distributions of the minimum Lorentz factor of electrons ($\gamma_{\rm min}$, *Panel* (a)), the break Lorentz factor of electrons ($\gamma_{\rm b}$, *Panel* (b)), the magnetic field strength (B, *Panel* (c)), and the beaming factor (δ, *Panel* (d)). The blazar data are taken from Zhang et al. (2012, 2014, 2015).

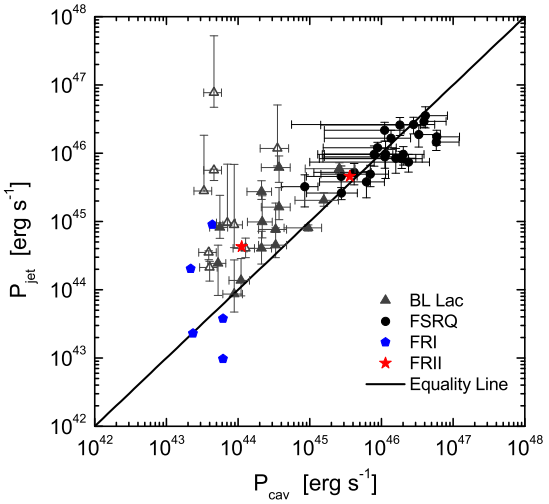

Fig. 3 Comparison between $P_{\rm jet}$ and $P_{\rm cav}$. The blue pentagons and red stars represent FR I and FR II RGs, respectively. The data on FSRQs (*black circles*) and BL Lacs (*dark-gray triangles*) from Zhang et al. (2014) are also presented, where the open dark-gray triangles are for BL Lacs with $\gamma_{\rm min} = 2$ as reported in Zhang et al. 2014. The solid line is the equality line.

a mean of $\sim 20^\circ$. This is roughly consistent with our results. Hovatta et al. (2009) also reported that the derived Doppler factors of RGs are much smaller than those of blazars, but the viewing angles are larger than those of blazars.

4.2 Jet Power and Cavity Kinetic Power

Based on the jet parameters of SED fitting and the assumption of $\Gamma = \delta$, we also calculate the jet power ($P_{\rm jet}$). It is assumed that the jet power of RGs is car-

ried by relativistic electrons, cold protons, magnetic fields and radiations, i.e., $P_{\rm jet} = \sum_i \pi R^2 \Gamma^2 c U_{\rm i}'$, where $U_i'(i = {\rm e},\ {\rm p},\ B, {\rm r})$ are the energy densities associated with the emitting electrons ($U_{\rm e}'$), cold protons ($U_{\rm p}'$), magnetic fields (U_B') and radiations ($U_{\rm r}'$) measured in the co-moving frame (Ghisellini et al. 2009). Following our and other author's works about blazars (e.g., Ghisellini et al. 2009; Zhang et al. 2012, 2014), the proton-electron pair assumption is also used here. The values of jet powers are also reported in Table 1. Note that the $\gamma_{\rm min}$ values of PKS 0625–35, Cen B and Pic A are taken as $\gamma_{\rm min} = 1$ in Table 1, which may overestimate the values of $P_{\rm jet}$. Hence we use $\gamma_{\rm min} = 300$ to calculate their jet powers and the powers of electrons and protons, where $\gamma_{\rm min} = 300$ is the median of the other nine GeV RGs.

The RGs always have large-scale jets, which are believed to be connected with their central engines (Harris & Krawczynski 2006). The observed X-ray cavities are evidence for AGN feedback and provide a direct measurement of the mechanical energy released by AGNs (Bîrzan et al. 2008; Cavagnolo et al. 2010). The cavity kinetic power is correlated with radio power on the large scale of galaxies (Bîrzan et al. 2004, 2008; Cavagnolo et al. 2010; O'Sullivan et al. 2011), and thus the cavity kinetic power ($P_{\rm cav}$) can be estimated using the relation between $P_{\rm cav}$ and radio luminosity. There are five FR I RGs (NGC 1218, NGC 1275, NGC 6251, M87 and Cen A) and two FR II RGs (3C 111 and 3C 380) in our sample with available $P_{\rm cav}$ in Meyer et al. (2011), as listed in Table 1. Comparison between $P_{\rm jet}$ and $P_{\rm cav}$ for the GeV RGs is given in Figure 3, and the data on FSRQs and BL Lacs from Zhang et al. (2014) are also presented. The distributions of RGs in the $P_{\rm cav}$–$P_{\rm jet}$ plane are roughly consistent with blazars; the five FR I RGs are in the low power end of BL Lacs, while one FR II RG overlaps with the distributions of FSRQs and another one overlaps with BL Lacs. However, with the small sample we cannot suggest that the FR I RGs are unified with BL Lacs and FR II RGs are unified with FSRQs in the $P_{\rm cav}$–$P_{\rm jet}$ plane.

4.3 Jet Composition and Radiation Efficiency

In order to investigate the jet composition and radiation efficiency of RGs, we also calculate the powers carried by each component: the powers of electrons ($P_{\rm e}$), protons ($P_{\rm p}$), magnetic fields (P_B) and radiations ($P_{\rm r}$). $P_{\rm e} + P_{\rm p}$ as a function of P_B, and $P_{\rm r}$ as the functions of $P_{\rm jet}$ and P_B are shown in Figure 4. The data of BL Lacs in Zhang et al. (2012) and FSRQs in Zhang et al. (2014, 2015) are also presented in Figure 4. Only FR I RG PKS 0625–35 has much higher P_B than its $P_{\rm e} + P_{\rm p}$ as shown in Figure 4(a). Therefore, the jets of RGs are likely dominated by particles. This is different from the results of blazars: the FSRQ jets are highly magnetized and the BL Lac jets are matter dominated (Zhang et al. 2014).

In the $P_{\rm jet}$–$P_{\rm r}$ plane, $P_{\rm r}$ for all the RGs is lower than their $P_{\rm jet}$, similar to blazars. The jet radiation efficiency $\epsilon_{\rm r} = P_{\rm r}/P_{\rm jet}$ for most of the GeV RGs is larger than 0.01, and the four FR II RGs have $\epsilon_{\rm r} > 0.1$, which is similar to FSRQs. On average, $\epsilon_{\rm r}$ of FR II RGs is higher than that of FR I RGs. One can also observe that $\epsilon_{\rm r}$ for most of the FSRQs ranges from 0.1 to 1 while $\epsilon_{\rm r}$ for most of the BL Lacs is between 0.01 and 0.1. In this respect, it seems that FR I RGs are unified with BL Lacs with low jet radiation efficiency while FR II RGs are unified with FSRQs with high jet radiation efficiency. In the P_B–$P_{\rm r}$ plane, RGs roughly follow the distributions of blazars along the equality line and extend to the low power end. These results may indicate a possible correlation between P_B and $P_{\rm r}$, suggesting that the radiation efficiency of a jet may be related with the jet magnetization for GeV RGs, analogous to blazars.

4.4 The Sequence in the $\nu_{\rm s} - P_{\rm jet}$ Plane

The 12 GeV RGs and the GeV blazars in our sample are shown in the $\nu_{\rm s} - L_{\rm s}$ plane in Figure 5(a), where $\nu_{\rm s}$ and $L_{\rm s}$ are the peak frequency and peak luminosity of their synchrotron radiation, respectively. No significant evidence is found for the trend associated with the "blazar sequence" [5] with or without the 12 GeV RGs. FSRQs and BL Lacs are clearly separated by $\nu_{\rm s} = 10^{14}$ Hz. The distribution of the four FR II RGs is marginally consistent with FSRQs, while the eight FR I RGs have $\nu_{\rm s}$ that is more similar to BL Lacs, but much lower luminosity than BL Lacs. Considering the different Doppler factors of these sources, we show the $\nu_{\rm s} - L_{\rm s}$ relation in the co-moving frame in Figure 5(b). Still no track of "blazar sequence" is found with or without the 12 GeV RGs. However, the phenomenon of "blazar envelope" suggested by Meyer et al. (2011) is observed for these GeV AGNs.

It becomes interesting if we replace $L_{\rm s}$ with the jet power ($P_{\rm jet}$) of sources, as displayed in Figure 5(c) and

[5] The increase of $\nu_{\rm s}$ corresponds to the decreases of luminosity (Fossati et al. 1998).

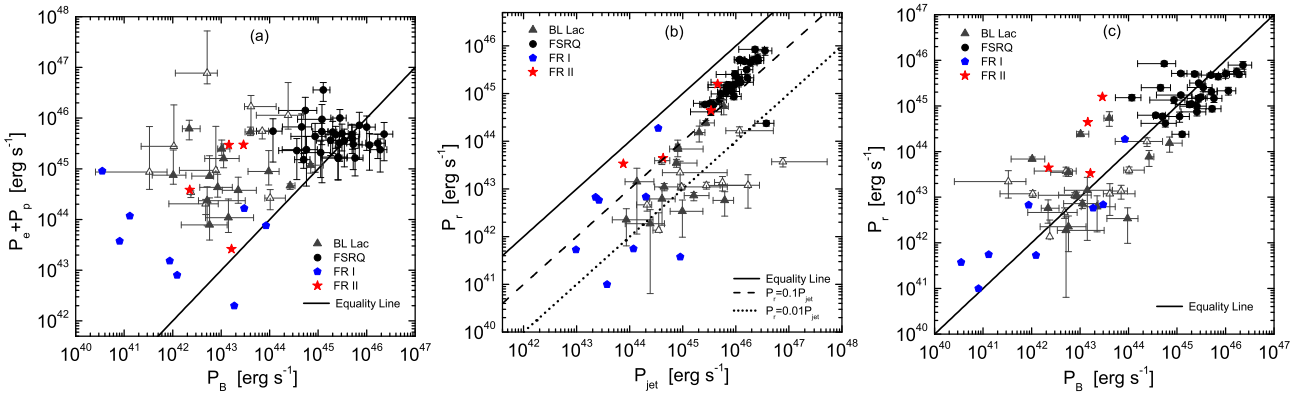

Fig. 4 (a) $P_{\rm e}+P_{\rm p}$ as a function of P_B, (b) $P_{\rm r}$ as functions of $P_{\rm jet}$ and (c) P_B. The black circles represent FSRQs from Zhang et al. (2014, 2015). The dark-gray triangles signify BL Lacs from Zhang et al. (2012) while the open dark-gray triangles are for BL Lacs with $\gamma_{\rm min}=2$ as reported in Zhang et al. 2014. The blue pentagons and red stars are for FR I and FR II RGs, respectively.

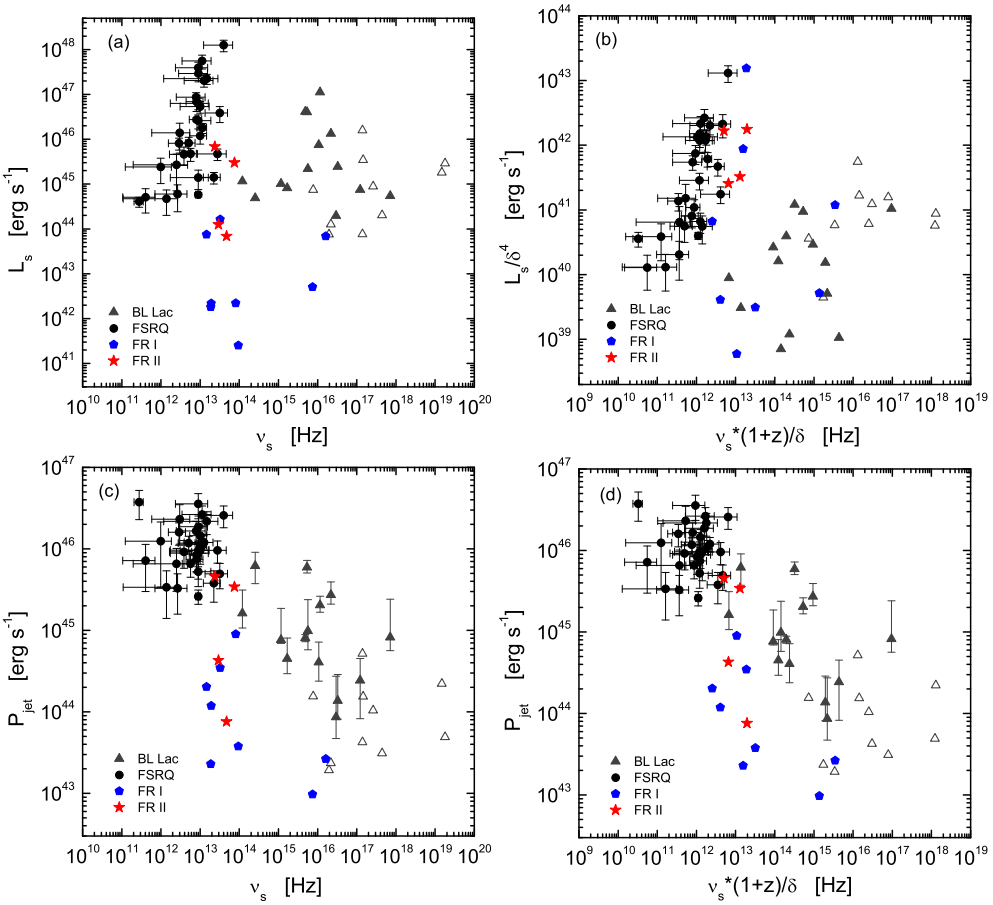

Fig. 5 Synchrotron peak luminosity ($L_{\rm s}$) and jet power ($P_{\rm jet}$) as a function of the synchrotron peak frequency ($\nu_{\rm s}$) in the observer (*Panels* (a) and (c)) and co-moving (*Panels* (b) and (d)) frames. Note that for BL Lacs with $\gamma_{\rm min}=2$ as reported in Zhang et al. (2014), their $P_{\rm jet}$ values are recalculated with $\gamma_{\rm min}=190$ and are marked as open triangles. For more details see Section 4.4.

(d). Note that the $\gamma_{\rm min}$ values for ten SEDs of BL Lacs are poorly constrained and taken as $\gamma_{\rm min}=2$ in Zhang et al. (2012), which may lead to significant overestimation of their $P_{\rm jet}$ as described in Section 4.2. So, we use the median of $\gamma_{\rm min}=190$ for the other 14 SEDs of BL Lacs to recalculate the $P_{\rm jet}$ values for the ten SEDs of BL Lacs, which are shown as open triangles without errors in Figure 5(c) and (d). A strong anticorrelation between $\nu_{\rm s}$ and $P_{\rm jet}$ is found for all the data points in the plane with a Pearson correlation coefficient $r=-0.69$

and a chance probability $p = 2.1 \times 10^{-10}$. After correcting the peak frequency into the co-moving frame, this correlation becomes even stronger, as displayed in Figure 5(d), with a Pearson correlation coefficient $r = -0.74$ and a chance probability $p = 2.1 \times 10^{-12}$. The distributions of the GeV RGs are roughly consistent with the distributions of these GeV blazars with slightly lower powers[6]. These results indicate that the "sequence" behavior among blazars, together with the GeV RGs, may be intrinsically dominated by the jet power, which means that the jet power regulates the synchrotron peak, as reported by Meyer et al. (2011).

5 SUMMARY

An SED sample of 12 GeV RGs is collected and compiled from the literature and NED. On the basis of jet parameters derived by SED fits with the one-zone leptonic model, we calculate the jet powers and the powers carried by each component to investigate their jet compositions and radiation efficiencies, as well as the relations between jet power and larger-scale kinetic power. We also present a comparison of jet properties between GeV RGs and blazars, where the data of blazars are taken from Zhang et al. (2012, 2014, 2015). Our results are summarized below.

- The observed SEDs of the 12 GeV RGs can be explained with the one-zone leptonic model, i.e., synchrotron + SSC model.
- Their distributions of B, $\gamma_{\rm b}$ and $\gamma_{\rm min}$ span the parameter spaces of BL Lacs and FSRQs. No significant unification is found for these jet parameters between FR I RGs and BL Lacs and between FR II RGs and FSRQs. However, on average FR I RGs have larger $\gamma_{\rm b}$ and lower B than FR II RGs, analogous to the differences between BL Lacs and FSRQs. The derived δ values of RGs are on average smaller than those of blazars, which is consistent with the unification model in which RGs are the misaligned parent populations of blazars with smaller Doppler factors.
- In the $P_{\rm cav}$–$P_{\rm jet}$ plane, the distributions of RGs are roughly consistent with blazars, and extend to the low power end.
- Most of the RG jets may be dominated by particles, but their jet radiation efficiencies could still be related to the extent of their jet magnetization. On average, the jet radiation efficiencies of FR II RGs are higher than those of FR I RGs.
- A strong anticorrelation between $\nu_{\rm s}$ and $P_{\rm jet}$ is observed for the GeV blazars and GeV RGs, and this correlation becomes stronger after correcting the peak frequency into the co-moving frame, indicating that the "sequence" behavior among blazars, together with the GeV RGs, may be intrinsically dominated by jet power.

[6] Although $P_{\rm cav}$ of RGs is lower than those of blazars in Figure 3, which may imply that RGs should have lower jet powers, we cannot report that the jet powers of RGs should be intrinsically lower than those of blazars with our limited sample of sources. The kinetic energy of X-ray cavities only provides a lower limit to the jet energy if shocks exist in the hot gas (Bîrzan et al. 2008). Hence, we propose that the lower jet powers of RGs should be affected by poor constraints on model parameters.

Acknowledgements We thank the anonymous referee for his/her valuable suggestions. We appreciate our helpful discussion with Ting-Feng Yi. This work is supported by the National Natural Science Foundation of China (grants 11573034, 11533003, 11373036 and 11133002), the National Basic Research Program (973 Program) of China (grant 2014CB845800) and the Guangxi Science Foundation (2013GXNSFFA019001).

References

Abdo, A. A., Ackermann, M., Ajello, M., et al. 2009a, ApJ, 699, 31
Abdo, A. A., Ackermann, M., Ajello, M., et al. 2009b, ApJ, 707, 55
Abdo, A. A., Ackermann, M., Ajello, M., et al. 2010a, ApJ, 720, 912
Abdo, A. A., Ackermann, M., Ajello, M., et al. 2010b, ApJ, 719, 1433
Abdo, A. A., Ackermann, M., Ajello, M., et al. 2010c, Science, 328, 725
Ackermann, M., Ajello, M., Atwood, W. B., et al. 2015, ApJ, 810, 14
Aharonian, F., Akhperjanian, A., Beilicke, M., et al. 2003, A&A, 403, L1
Aharonian, F., Akhperjanian, A. G., Bazer-Bachi, A. R., et al. 2006, Science, 314, 1424
Aharonian, F., Akhperjanian, A. G., Anton, G., et al. 2009, ApJ, 695, L40
Aleksić, J., Antonelli, L. A., Antoranz, P., et al. 2010, ApJ, 723, L207
Aleksić, J., Alvarez, E. A., Antonelli, L. A., et al. 2012, A&A, 539, L2

Aleksić, J., Antonelli, L. A., Antoranz, P., et al. 2014, A&A, 563, A91
Baldi, R. D., & Capetti, A. 2009, A&A, 508, 603
Bartoli, B., Bernardini, P., Bi, X. J., et al. 2016, ApJS, 222, 6
Baum, S. A., Heckman, T. M., Bridle, A., van Breugel, W. J. M., & Miley, G. K. 1988, ApJS, 68, 643
Bîrzan, L., Rafferty, D. A., McNamara, B. R., Wise, M. W., & Nulsen, P. E. J. 2004, ApJ, 607, 800
Bîrzan, L., McNamara, B. R., Nulsen, P. E. J., Carilli, C. L., & Wise, M. W. 2008, ApJ, 686, 859
Buttiglione, S., Capetti, A., Celotti, A., et al. 2009, A&A, 495, 1033
Cavagnolo, K. W., McNamara, B. R., Nulsen, P. E. J., et al. 2010, ApJ, 720, 1066
Chen, L., Cao, X., & Bai, J. M. 2012, ApJ, 748, 119
Cui, Y.-D., Yuan, Y.-F., Li, Y.-R., & Wang, J.-M. 2012, ApJ, 746, 177
Fanaroff, B. L., & Riley, J. M. 1974, MNRAS, 167, 31P
Fossati, G., Maraschi, L., Celotti, A., Comastri, A., & Ghisellini, G. 1998, MNRAS, 299, 433
Franceschini, A., Rodighiero, G., & Vaccari, M. 2008, A&A, 487, 837
Fukazawa, Y., Finke, J., Stawarz, Ł., et al. 2015, ApJ, 798, 74
Fukazawa, Y., Shiki, K., Tanaka, Y., Itoh, R., & Nagai, H. 2016, arXiv:1608.03652
Ghisellini, G., Maraschi, L., & Dondi, L. 1996, A&AS, 120, 503
Ghisellini, G., Tavecchio, F., & Ghirlanda, G. 2009, MNRAS, 399, 2041
Hardcastle, M. J., Evans, D. A., & Croston, J. H. 2007, MNRAS, 376, 1849
Hardcastle, M. J., Evans, D. A., & Croston, J. H. 2009, MNRAS, 396, 1929
Harris, D. E., & Krawczynski, H. 2006, ARA&A, 44, 463
Hartman, R. C., Bertsch, D. L., Bloom, S. D., et al. 1999, ApJS, 123, 79
Hine, R. G., & Longair, M. S. 1979, MNRAS, 188, 111
Hovatta, T., Valtaoja, E., Tornikoski, M., & Lähteenmäki, A. 2009, A&A, 494, 527
Kataoka, J., Reeves, J. N., Iwasawa, K., et al. 2007, PASJ, 59, 279
Katsuta, J., Tanaka, Y. T., Stawarz, Ł., et al. 2013, A&A, 550, A66
Laing, R. A., Jenkins, C. R., Wall, J. V., & Unger, S. W. 1994, in Astronomical Society of the Pacific Conference Series, 54, The Physics of Active Galaxies, eds. G. V. Bicknell, M. A. Dopita, & P. J. Quinn, 201
Liao, N. H., Bai, J. M., Liu, H. T., et al. 2014, ApJ, 783, 83
Maraschi, L., Ghisellini, G., & Celotti, A. 1992, ApJ, 397, L5
McKinley, B., Yang, R., López-Caniego, M., et al. 2015, MNRAS, 446, 3478
Meyer, E. T., Fossati, G., Georganopoulos, M., & Lister, M. L. 2011, ApJ, 740, 98
Migliori, G., Grandi, P., Torresi, E., et al. 2011, A&A, 533, A72
Morganti, R., Killeen, N. E. B., & Tadhunter, C. N. 1993, MNRAS, 263, 1023
O'Sullivan, E., Giacintucci, S., David, L. P., et al. 2011, ApJ, 735, 11
Owen, F. N., & Laing, R. A. 1989, MNRAS, 238, 357
Saripalli, L. 2012, AJ, 144, 85
Sikora, M., Begelman, M. C., & Rees, M. J. 1994, ApJ, 421, 153
Sikora, M., Stawarz, Ł., Moderski, R., Nalewajko, K., & Madejski, G. M. 2009, ApJ, 704, 38
Tavecchio, F., Maraschi, L., & Ghisellini, G. 1998, ApJ, 509, 608
Tanaka, Y. T., Doi, A., Inoue, Y., et al. 2015, ApJL, 799, L18
Tavecchio, F., & Ghisellini, G. 2014, MNRAS, 443, 1224
Urry, C. M., & Padovani, P. 1995, PASP, 107, 803
Wu, Q., & Cao, X. 2008, ApJ, 687, 156
Xu, Y.-D., Cao, X., & Wu, Q. 2009, ApJ, 694, L107
Zhang, J., Bai, J. M., Chen, L., & Liang, E. 2010, ApJ, 710, 1017
Zhang, J., Bai, J.-M., Chen, L., & Yang, X. 2009, ApJ, 701, 423
Zhang, J., Liang, E.-W., Zhang, S.-N., & Bai, J. M. 2012, ApJ, 752, 157
Zhang, J., Sun, X.-N., Liang, E.-W., et al. 2014, ApJ, 788, 104
Zhang, J., Xue, Z.-W., He, J.-J., Liang, E.-W., & Zhang, S.-N. 2015, ApJ, 807, 51
Zhu, Y.-K., Zhang, J., Zhang, H.-M., et al. 2016, RAA (Research in Astronomy and Astrophysics), 16, 170
Zirbel, E. L., & Baum, S. A. 1995, ApJ, 448, 521